

Probing Local Electronic Anisotropy Using Anomalous Scattering Diffraction: $\text{Cs}_2[\text{AuCl}_2][\text{AuCl}_4]$

Angus P. Wilkinson

School of Chemistry and Biochemistry, Georgia Institute of Technology, Atlanta, Georgia 30332-0400

and

Lieselotte K. Templeton and David H. Templeton

Department of Chemistry, University of California, Berkeley, California 94720

Received February 7, 1995; accepted April 6, 1995

Resonant X-ray scattering tensors are derived for the two independent gold atoms in Wells' salt ($\text{Cs}_2[\text{AuCl}_2][\text{AuCl}_4]$) from diffraction intensities measured at several wavelengths near the Au L_{III} absorption edge using linearly polarized synchrotron radiation. The scattering behavior is very different for the two sites as a consequence of their distinct oxidation states and coordination environments. A π -polarized resonance for the Au(III) leads to a highly anisotropic tensor for this site; the scattering amplitude changes with polarization direction by as much as 7 electron units. Such measurements are equivalent to obtaining polarization-dependent X-ray absorption spectra for the individual crystallographic sites in materials with several distinct sites. Cesium gold chloride, $\text{Cs}_2\text{Au}_2\text{Cl}_6$, $M_r = 872.5$, tetragonal, $I4/mmm$, $a = 7.497(2)$, $c = 10.885(2)$ Å, $V = 611.8$ Å³, $Z = 2$, $D_x = 4.736$ g cm⁻³, $\lambda(\text{MoK}\alpha) = 0.71073$ Å, $\mu = 310$ cm⁻¹, $F(000) = 740$, $T = 295$ K, $R = 0.023$ for 247 reflections with $I > \sigma$. © 1995

Academic Press, Inc.

INTRODUCTION

Wells' salt, $\text{Cs}_2\text{Au}_2\text{Cl}_6$, has been known for many years. Its structure was originally examined by Elliott and Pauling with powder X-ray diffraction and it was found to be related to that of perovskite (1). It is distorted from that of an ideal perovskite by the presence of a commensurate static charge density wave that produces two distinct gold sites (see Fig. 1) linked by bridging chloride ions. One of these sites has square planar coordination and the other has linear coordination, formally corresponding to the presence of Au(III) and Au(I), respectively. The compound is a Robin and Day class II mixed-valence material (2).

In the last twenty-five years the isostructural (3) mixed-valence gold halides, $\text{Cs}_2\text{Au}_2\text{X}_6$ ($X = \text{Cl}, \text{Br}, \text{and I}$) have received considerable attention. This is a consequence of their electrical properties and the phase transitions that

they display at high pressures. An array of techniques has been employed to study these compounds, including single-crystal X-ray diffraction both under ambient conditions (4) and at high pressure (5), high-pressure energy dispersive X-ray diffraction (6, 7), high-pressure neutron diffraction (8), atmospheric-pressure (9–11) and high-pressure (12–14) ¹⁹⁷Au Mössbauer spectroscopy, X-ray photoelectron spectroscopy (15), conductivity measurements as a function of pressure (16–19), optical spectroscopy (20), ESR spectroscopy (21), band structure calculations (22–24), and X-ray absorption spectroscopy (25).

When the initially tetragonal $\text{Cs}_2\text{Au}_2\text{Cl}_6$ is placed under hydrostatic pressure at room temperature its resistivity drops by nine orders of magnitude between atmospheric pressure and 10 GPa (18). This decrease has been shown by single-crystal X-ray diffraction (5) to be associated with the movement of the bridging chloride ions toward the midpoints between neighboring gold sites and a change in electrical behavior from semiconducting to metallic at around 6 GPa (18). At about 5.2 GPa the two gold sites are equivalent by X-ray diffraction but the structure is still tetragonal. This is consistent with a Jahn–Teller type of distortion of Au(II) (d^9) in the structure (19). However, high-pressure low-temperature ¹⁹⁷Au Mössbauer spectroscopy suggests that there are still two distinct gold environments in the compound at pressures up to 6.8 GPa (13, 14). Very little work has been done on the corresponding bromide.

The high-pressure behavior of $\text{Cs}_2\text{Au}_2\text{I}_6$ has been explored in more detail than that of the chloride or bromide. It shows a semiconductor to metal transition (tetragonal to tetragonal) at about 5 GPa and room temperature (7, 16) and a further metal to metal transition (tetragonal to cubic) at about 6.5 GPa and 350 K (7, 16). Remarkably, the high-pressure cubic phase is metastable at atmospheric

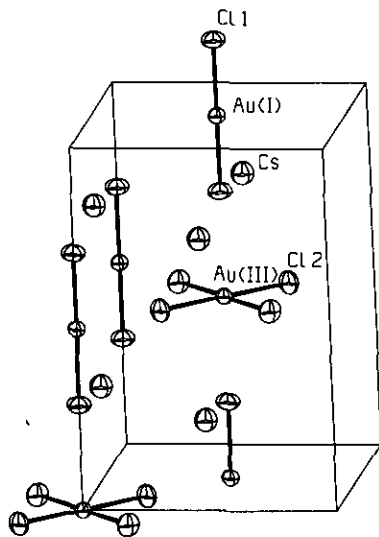


FIG. 1. The structure of $\text{Cs}_2\text{Au}^{\text{I}}\text{Au}^{\text{III}}\text{Cl}_6$.

pressure and room temperature (16). ^{197}Au Mössbauer studies on quenched material (11) indicate the presence of a single gold site in the cubic phase. High-pressure Mössbauer work (12) at low temperature (4.2 K) shows that the difference between the two gold environments decreases as the pressure is increased, and at high pressures (12.5 GPa) there is only one gold environment. The sites become equivalent somewhere between 6.6 and 12.5 GPa.

Spectroscopic experiments on compounds with more than one environment for a given element, such as $\text{Cs}_2\text{Au}_2\text{Cl}_6$, produce spectra that are averages over the different environments and orientations in the solid. While techniques such as X-ray absorption spectroscopy are potentially powerful tools for obtaining local structural and electronic parameters, much of this information is lost when the spectra are averaged. In the case of crystalline materials and X-ray absorption spectroscopy it is possible to overcome this limitation by combining the "absorption measurement" with a crystallographic experiment.

The X-ray scattering factor of an atom is not independent of the incident radiation's energy. The variation with energy is described by the anomalous scattering terms $f'(E)$ and $f''(E)$, which are closely related to the X-ray absorption cross section for the atom responsible for the scattering. It has been demonstrated by several workers that it is possible to obtain estimates of $f'(E)$ and $f''(E)$ from crystallographic data for compounds containing multiple environments for an element. The samples studied have included mixed-valence compounds such as Eu_3O_4 (26), GaCl_2 (27, 28), $\text{YB}_2\text{Cu}_3\text{O}_{7.8}$ (29–31), $\alpha\text{-Fe}_2\text{PO}_5$ (32), $(\mu\text{-dioxo})(\text{Mn}-(2,2'\text{-bipyridyl})_2)_2(\text{BF}_4)_3 \cdot 3\text{H}_2\text{O}$ (33), Co_3O_4 (34), and materials with multiple coordination

environments for the element in a single oxidation state, for example, $\text{Y}_3\text{Ga}_5\text{O}_{12}$ (35). These experiments are in many ways equivalent to performing a crystallographic site-specific X-ray absorption measurement. Some of the work that has been done has employed an EXAFS-style analysis of the fine structure that is seen in the diffraction data as a consequence of the variation of f' and f'' with energy (31, 34, 36, 37). This fine structure is usually referred to DAFS (diffraction anomalous fine structure).

It is well known that the X-ray absorption spectra of many materials display a dependence on the polarization of the incident photons as a consequence of an anisotropic coordination environment around the absorbing site(s). As the energy-dependent component of the scattering factor is closely related to the X-ray absorption coefficient, it is also dependent on the beam polarization. Diffraction experiments can be used to look at the polarization dependence of an absorbing site even when the material is macroscopically isotropic (38, 39) or the sample is in powder form (34)! For example, the polarization dependence of the scattering from Br in NaBrO_3 has been examined (38). In this case the local environment around the absorber (BrO_3^-) is highly anisotropic but the crystals are cubic and hence macroscopically isotropic.

ANISOTROPY OF DIFFRACTION

In the dipole approximation, the resonant scattering factor of an anisotropic atom is a tensor of second rank (39–41). For an atom in a site of uniaxial symmetry this tensor can be represented by a matrix,

$$\mathbf{f} = \begin{pmatrix} f_0 + f'_\pi + if''_\pi & 0 & 0 \\ 0 & f_0 + f'_\pi + if''_\pi & 0 \\ 0 & 0 & f_0 + f'_\sigma + if''_\sigma \end{pmatrix}. \quad [1]$$

For each combination of unit polarization vectors \mathbf{e}_1 and \mathbf{e}_2 of incident and scattered rays the amplitude scattered by the atom is $f = \mathbf{e}_2^T \mathbf{f} \mathbf{e}_1$. The parameters in this matrix, which are sensitive functions of wavelength, can be derived from intensities measured in diffraction experiments with polarized X-rays and a variety of crystal orientations.

In the crystal structure of $\text{Cs}_2\text{Au}_2\text{Cl}_6$ (1, 4) (Fig. 1) each kind of Au atom is in a special position that requires the unique direction of its uniaxial tensor to lie along the crystallographic c axis. For l even, the structure factor depends on the sum of the two tensors; for l odd, it depends on the difference. Thus to determine the individual tensors one needs data for both even and odd l values. As in K_2PtCl_4 (42) there is an orientation for each hkl (called the " π setting"), for which the

TABLE 1
Diffraction Experiments and Resulting Tensors

<i>E</i> (eV)	11914.7	11920.9	11922.5	11923.1	11924.9	11928.3
<i>N</i>	187	439	230	141	197	364
<i>R</i> (%)	3.5	4.7	3.7	4.2	4.3	4.8
<i>K</i>	-0.025	-0.190	-0.220	-0.380	-0.355	-0.010
θ_{\max}	65	77	45	35	77	77
l_{\max}	1	3	3	3	1	3
Au(I)						
f_{π}^{σ}	-16.7(3)	-18.2(2)	-18.7(2)	-17.9(3)	-16.1(5)	-17.2(2)
f_{σ}^{σ}	-16.7(3)	-18.6(1)	-19.2(2)	-18.9(2)	-17.2(3)	-17.7(2)
f_{π}^{π}	4.5(5)	5.4(2)	5.8(3)	6.0(3)	7.0(7)	9.1(5)
f_{σ}^{π}	3.9(8)	6.9(4)	8.2(3)	7.8(4)	8.7(5)	9.7(3)
Au(III)						
f_{π}^{σ}	-18.2(2)	-20.8(1)	-20.9(2)	-19.9(3)	-14.0(5)	-14.5(2)
f_{σ}^{σ}	-16.3(2)	-17.9(1)	-18.3(2)	-18.3(2)	-18.7(3)	-18.2(2)
f_{π}^{π}	6.0(5)	8.4(2)	9.9(2)	11.0(3)	12.9(6)	6.9(4)
f_{σ}^{π}	4.7(7)	5.0(3)	5.4(3)	5.4(3)	5.5(5)	6.3(2)

Note. $R = \sum |\Delta F| / \sum |F_0|$ for *N* observations; *K* is the parameter for dichroism.

scattering of linearly polarized radiation depends only on the π components of the tensors. There is also a "σ setting," 90° in azimuth from the π setting, for which the scattering depends to the greatest extent on the σ components. Only in the case of *hk0* reflections is this σ dependence complete.

EXPERIMENTAL

A sample of $\text{Cs}_2\text{Au}^{\text{I}}\text{Au}^{\text{III}}\text{Cl}_6$ was prepared using a procedure closely related to that of Wells (43). Under flowing nitrogen 4.85 g of HAuCl_4 was heated to 225°C. This produced a mixture of AuCl and some gold metal. Then 19.86 g of CsCl dissolved in a small amount of 1:1 hydrochloric acid was added to the thermal decomposition products and the mixture was boiled. A further 250 cm³ of 1:1 hydrochloric acid was then added and the mixture was heated again so that the initially formed black solid ($\text{Cs}_2\text{Au}_2\text{Cl}_6$) dissolved, leaving behind the gold metal. The solution was decanted and allowed to cool. The initially recovered small crystals were subsequently recrystallized from a solution containing 5 g CsCl in 50 cm³ of 1:1 hydrochloric acid.

A crystal (.09 × .15 × .22 mm with 9 faces) was selected and glued to a glass fiber. Intensities of 938 nonzero reflections (264 independent) with $\theta < 30^\circ$ were measured with $\text{MoK}\alpha$ radiation using an Enraf-Nonius CAD-4 diffractometer. Transmission factors calculated by analytical integration ranged from 0.057 to 0.12. Extinction reduced some intensities by more than a factor of 3, and 17 strong reflections were deleted. An empirical correction for extinction in the least-squares refinement increased the F_0 of the strongest remaining reflection by

37%. Atomic scattering factors were taken from International Tables for X-ray Crystallography (44) with dispersion corrections for all atoms calculated with the program of Cromer (45). A full-matrix least-squares refinement was carried out, minimizing $\sum w(|F_0| - |kF_c|)^2$, where *k* is a scaling factor, $w = [\sigma'(F)]^{-2}$, $\sigma'(F^2) = ([\sigma(F^2)]^2 + [0.04 \times F^2]^2 + [5.0]^2)^{1/2}$, and $\sigma(F^2)$ is obtained from counting statistics. The final cycle of refinement converged, giving $R_w = 0.026$ and $R = 0.023$. The atomic coordinates (Cl(1), $z = 0.2904(3)$; Cl(2), $x = 0.2165(2)$) agree with those of Tindemans-Van Eindhoven and Verschoor (4). Observed and calculated structure factors for this refinement, and anisotropic temperature factors are available as supplementary material.¹ Our thermal displacement parameters are on average about 10% larger than those previously reported, perhaps because of a different amount and treatment of absorption and extinction. Extinction is not mentioned in the previous work.

The same crystal was used at the SSRL (Stanford Synchrotron Radiation Laboratory) on Line 1-5 (a bending-magnet line with a Si(111) double-crystal monochromator and no focusing, 40-90 mA ring current at 3 GeV) with a CAD-4 diffractometer (46), ω -scan range of 0.3° or 0.5°, and scan time of 30 sec or less. Each reflection in one octant of reciprocal space, starting with $l = 0$ and up to the maximum l and θ stated in Table 1, was measured at the π and σ azimuthal settings described above. Measurements were deleted if too weak for good counting statistics, if too strong for the detector, if repeated scans failed to check, or if extinction was excessive. After normalization for beam intensity according to an ion chamber, periodic measurements of a standard reflection varied by as much as 23%. Four of the six data sets were adjusted for these changes by interpolation. Since the ion chamber intercepts more of the beam than does the crystal, it is less sensitive to shifts of the beam position. Transmission factors calculated by analytical integration (assuming isotropic absorption) ranged from 0.019 to 0.14. The effect of dichroism on transmission was estimated as described by Templeton and Templeton (47) using the empirical *K* values listed in Table 1. The photon energy scale is based on 11.9212 keV for the *K*-edge inflection of metallic Au (48). In addition to the diffraction measurements, polarization-dependent absorption spectra, measured using a

¹ See NAPS document No. 05223 for 3 pages of supplementary material. Order from ASIS/NAPS. Microfiche Publications, P.O. Box 3513, Grand Central Station, New York, NY 10163. Remit in advance \$4.00 for microfiche copy or for photocopy, \$7.75 up to 20 pages plus \$3.00 for each additional page. All orders must be prepaid. Institutions and organizations may order by purchase order. However, there is a billing and handling charge for this service of \$15. Foreign orders add \$4.50 for postage and handling, for the first 20 pages, and \$1.00 for each additional 10 pages of material, \$1.50 for postage of any microfiche orders.

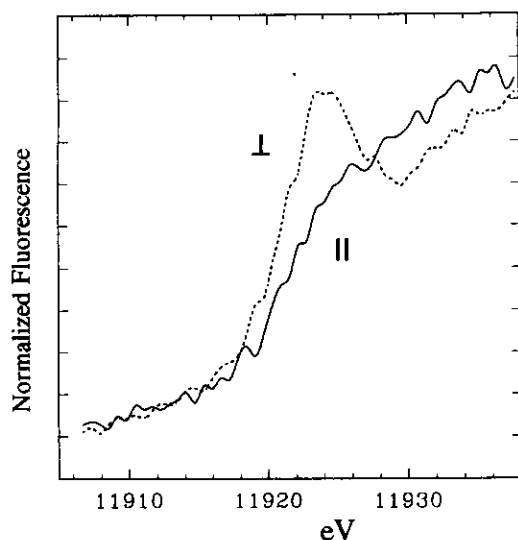


FIG. 2. Au L_{III} fluorescence spectra of Cs₂Au^IAu^{III}Cl₆ measured parallel and perpendicular to the crystallographic *c* axis.

fluorescence technique, were recorded for the single crystal of Cs₂Au₂Cl₆ while it was mounted on the diffractometer (Fig. 2).

Eight tensor components and a scale factor were determined by least-squares analysis of each synchrotron data set with all the structural parameters fixed at the values determined from the MoK α data. An extinction parameter and the dichroism parameter *K* were determined by trial and error. Care was necessary in the choice of initial f''

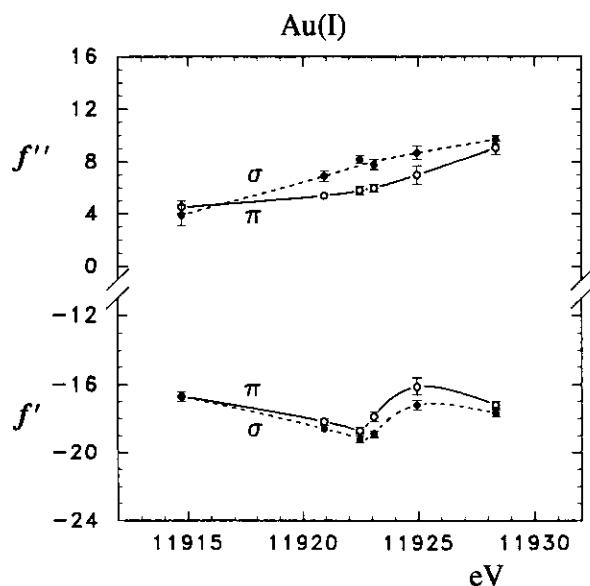


FIG. 3. The real and imaginary parts of the anomalous scattering tensor for the Au(I) site. The open circles are the π component and the closed circles are the σ component.

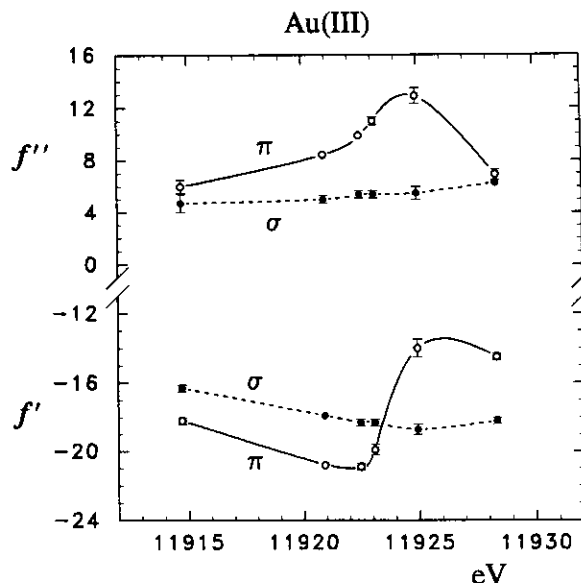


FIG. 4. The real and imaginary parts of the anomalous scattering tensor for the Au(III) site. The open circles are the π component and the closed circles are the σ component.

values because with some of the data sets a local minimum exists for interchange of f''_{σ} for the two Au atoms. The agreement of F_o and F_c was not as good when the parameters of Tindemans-Van Eijndhoven and Verschoor (4) were used. The results are listed in Table 1 and plotted in Figs. 3 and 4.

DISCUSSION

An examination of Figs. 3 and 4 shows that the two gold sites have very different scattering behavior. In the case of the Au(I) site there is a modest anisotropy which corresponds with somewhat stronger resonance absorption for polarization along the crystallographic *c* direction. The scattering factor tensor for the Au(III) site is highly anisotropic with behavior in the *a*-*b* plane that is markedly different from that observed for the Au(I). In particular, the pronounced peak in f''_{π} , along with the corresponding derivative-like feature in f'_{π} , at about 11925 eV implies the presence of a strongly π -polarized transition at this energy for the Au(III). It should be noted that f'' is linearly related to the photoelectric absorption cross section, σ , ($f'' \propto \sigma E$) and $f'(E)$ is connected to $f''(E)$ via the Kramers-Kronig relationship (49, 50).

The above observations are consistent with both our polarized fluorescence spectra obtained for a single crystal sample of Cs₂Au₂Cl₆ and the unpolarized X-ray absorption experiments performed on the salts Bu₄NAuCl₄ and Bu₄NAuCl₂, by Tanino and Takahashi (25). Our fluorescence spectra show a π -polarized (in the crystallographic

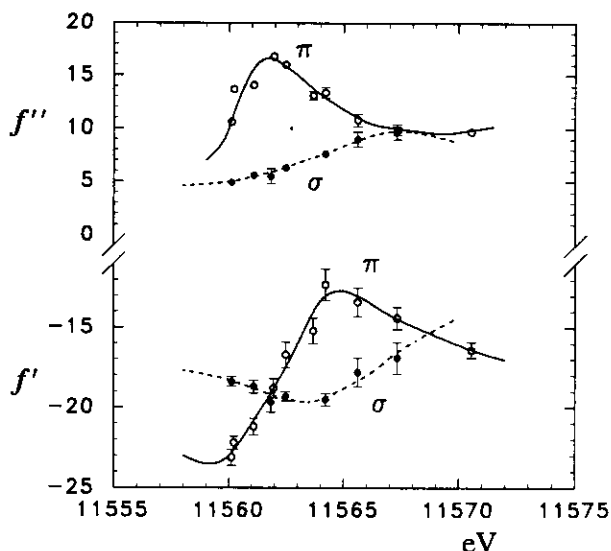


FIG. 5. The real and imaginary parts of the anomalous scattering tensor for Pt(II) in K_2PtCl_4 (42). The open circles are the π component and the closed circles are the σ component.

a - b plane) resonance at 11924 eV (Fig. 2) and the unpolarized studies on the butyl ammonium salts show that only the Au(III) compound has a strong pre-edge transition.

The presence and origin of strong near-edge features in the L_{III} spectra of many transition metal complexes is well established. The transitions are thought to be localized $2p \rightarrow nd$ in nature (51) and the magnitude of the "white line" or pre-edge feature is related to the d orbital occupancy at the metal site (52, 53). Consequently, a d^{10} ion like Au(I) is not expected to show a significant pre-edge feature, but Au(III), which is d^8 , should show a pre-edge feature. For a square planar d^8 metal complex the lowest unoccupied orbital is the $d_{x^2-y^2}$. In the case of $Cs_2Au_2Cl_6$, this vacant orbital lies in the crystallographic a - b plane, giving rise to a $2p \rightarrow 5d_{x^2-y^2}$ transition polarized in this plane (51).

It is interesting to compare our determination of the tensor components for Au(III) in $Cs_2Au_2Cl_6$ with those previously determined for Pt(II) in K_2PtCl_4 (see Figs. 4 and 5) (42). The general features of the two sets of measurements are the same. However, the maximum in $f''_{\pi}(E)$ for the gold compound is not as great as that for the platinum compound, and the minimum in $f'_{\pi}(E)$ is not as low for the gold compound as it was for the platinum compound. These differences are too large to be a consequence of experimental errors. However, an explanation can be found in the electronic structures of the compounds. The pre-edge feature observed for Pt(II) compounds, such as PtI_2 , is often stronger than that found for Au(III) compounds, like $AuCl_3$ (53). This difference can be rationalized by considering d orbital occupancies.

While both compounds have a formal d^8 electron configuration, the vacant orbital involved in the pre-edge transition is not purely metal d in character; it also has a contribution from the ligand orbitals. It is likely that the metal d orbitals will be lower in energy in the Au(III) complex than in the Pt(II) complex due to the higher formal oxidation state of the gold, consequently the LUMO (lowest unoccupied molecular orbital) for the gold complex will have less metal d character than the LUMO for the platinum complex. This increased d orbital occupancy in the case of the gold compound leads to the lower intensity of the pre-edge feature and to the differences observed between the anomalous scattering behaviour for the Au(III) and Pt(II) species.

Our experiment demonstrates that it is possible, using anomalous scattering diffraction, to obtain site-specific information about the anisotropy of the local electronic environment of atoms in solids containing more than one type of environment. Anomalous scattering diffraction is potentially a very useful approach as more information is available from this experiment than from a simple combination of crystallography and polarized X-ray absorption spectroscopy. We have only determined the components of the scattering tensors at a small number of energies in the vicinity of the absorption edge, however, it is now feasible to determine their values at many different energies in a reasonable amount of time. This could be done using either scanning monochromator techniques or by employing an over-bent focusing monochromator and a position-sensitive detector (54-56). The former approach has already been employed for DAFS experiments on simpler compounds than the one discussed in this paper (31, 34, 36, 37). With recent and projected advances in both synchrotron radiation sources and instrumentation many exciting experiments that combine the power of X-ray absorption and diffraction in a synergistic fashion will soon be possible.

ACKNOWLEDGMENTS

We thank the many staff members of the Stanford Synchrotron Radiation Laboratory (SSRL) whose assistance made this work possible. We are particularly indebted to Dr. Michael Soltis. This research was in part performed at SSRL, which is operated by the Department of Energy, Office of Basic Energy Sciences. The SSRL Biotechnology Program is supported by the NIH, Biomedical Resource Technology Program, Division of Research Resources. Further funding for SSRL is provided by the Department of Energy, Office of Health and Environmental Research. Part of this work was supported by Shell, KSLA, Amsterdam and the Georgia Institute of Technology.

REFERENCES

1. N. Elliott and L. Pauling, *J. Am. Chem. Soc.* **60**, 1846 (1938).
2. M. B. Robin and P. Day, *Adv. Inorg. Chem. Radiochem.* **10**, 247 (1967).

3. G. Brauer and G. Sleater, *J. Less-Common Met.* **21**, 283 (1970).
4. J. C. M. Tindemans-v. Eijndhoven and G. C. Verschoor, *Mater. Res. Bull.* **9**, 1667 (1974).
5. W. Denner, H. Schulz, and H. D'Amour, *Acta Crystallogr.* **A35**, 360 (1979).
6. H. Kitagawa, H. Sato, and N. Kojima, *Synth. Met.* **41-43**, 1953 (1991).
7. H. Kitagawa, H. Sato, N. Kojima, T. Kikegawa, and O. Shimomura, *Solid State Commun.* **78**, 989 (1991).
8. P. Day, C. Vettier, and G. Parisot, *Inorg. Chem.* **17**, 2319 (1978).
9. M. Katada, Y. Uchida, K. Sato, H. Sano, H. Sakai, and Y. Maeda, *Bull. Chem. Soc. Jpn.* **55**, 444 (1982).
10. H. Kitagawa, N. Kojima, and H. Sakai, *J. Chem. Soc. Dalton Trans.*, 3211 (1991).
11. N. Kojima, F. Amita, H. Kitagawa, H. Sakai, and Y. Maeda, *Nucl. Instrum. Methods Phys. Res. Sect. B* **76**, 321, (1993).
12. S. S. Hafner, N. Kojima, J. Stanek, and L. Zhang, *Phys. Lett. A* **192**, 385 (1994).
13. J. Stanek, S. S. Hafner, and H. Schulz, *Phys. Lett. A* **76**, 333 (1980).
14. J. Stanek, *J. Chem. Phys.* **76**, 2315 (1982).
15. H. Kitagawa, N. Kojima, and T. Nakajima, *J. Chem. Soc. Dalton Trans.*, 3121 (1991).
16. N. Kojima, H. Kitagawa, T. Ban, F. Amita, and M. Nakahara, *Solid State Commun.* **73**, 743 (1990).
17. N. Kojima, H. Kitagawa, T. Ban, F. Amita, and M. Nakahara, *Synth. Met.* **41-43**, 2347 (1991).
18. R. Keller, J. Fenner, and W. B. Holzapfel, *Mater. Res. Bull.* **9**, 1363 (1974).
19. H. Kitagawa, N. Kojima, H. Takahashi, and N. Mori, *Synth. Met.* **55-57**, 1726 (1993).
20. N. Kojima and H. Kitagawa, *J. Chem. Soc. Dalton Trans.*, 327 (1994).
21. H. Kitagawa, N. Kojima, N. Matsushita, T. Ban, and I. Tsujikawa, *J. Chem. Soc. Dalton Trans.*, 3115 (1991).
22. R. Allub and B. Alascio, *Solid State Commun.* **85**, 99 (1993).
23. J. A. Paradis, M.-H. Whangbo, and R. V. Kasowski, *New J. Chem.* **17**, 525 (1993).
24. M. Shirai, *Synth. Met.* **55-57**, 3389 (1993).
25. H. Tanino and K. Takahashi, *Solid State Commun.* **59**, 825 (1986).
26. J. P. Attfield, *Nature* **343**, 46 (1990).
27. A. P. Wilkinson, A. K. Cheetham, and D. E. Cox, *Acta Crystallogr. Sect. B* **47**, 155 (1991).
28. A. P. Wilkinson and A. K. Cheetham, *J. Appl. Crystallogr.* **25**, 654 (1992).
29. G. H. Kwei, R. B. Von Dreele, A. Williams, J. A. Goldstone, A. C. Lawson II, and W. K. Warburton, *J. Mol. Struct.* **223**, 383 (1990).
30. J. P. Attfield, *J. Phys. Chem. Solids* **52**, 1243 (1991).
31. L. B. Sorensen, J. O. Cross, M. Newville, *et al.*, in "Resonant Anomalous X-ray Scattering: Theory and Applications," (G. Materlik, C. J. Sparks, and K. Fischer, Eds.), p. 389. North-Holland, Amsterdam, 1994.
32. J. K. Warner, A. K. Cheetham, D. E. Cox, and R. B. Von Dreele, *J. Am. Chem. Soc.* **114**, 6074 (1992).
33. Y. Gao, A. Frost-Jensen, M. R. Pressprich, P. Coppens, A. Marquez, and M. Dupuis, *J. Am. Chem. Soc.* **114**, 9214 (1992).
34. I. J. Pickering, M. Sansone, J. Marsch, and G. N. George, *J. Am. Chem. Soc.* **115**, 6302 (1993).
35. D. E. Cox, and A. P. Wilkinson, in "Resonant Anomalous X-ray Scattering: Theory and Applications," (G. Materlik, C. J. Sparks, and K. Fischer, Eds.), p. 195. North-Holland, Amsterdam, 1994.
36. I. J. Pickering, M. Sansone, J. Marsch, and G. N. George, *Jpn. J. Appl. Phys.* **32** (suppl. 32-2), 206 (1993).
37. H. Stragier, J. O. Cross, J. J. Rehr, L. B. Sorensen, C. E. Bouldin, and J. C. Woicik, *Phys. Rev. Lett.* **69**, 3064 (1992).
38. D. H. Templeton and L. K. Templeton, *Acta Crystallogr. A* **41**, 133 (1985).
39. V. E. Dmitrienko, *Acta Crystallogr. A* **40**, 89 (1984).
40. D. H. Templeton and L. K. Templeton, *Acta Crystallogr. A* **38**, 62 (1982).
41. V. E. Dmitrienko, *Acta Crystallogr. A* **39**, 29 (1983).
42. D. H. Templeton and L. K. Templeton, *Acta Crystallogr. A* **41**, 365 (1985).
43. H. L. Wells, *Am. J. Sci.* [**5**] **3**, 315 (1922).
44. "International Tables for X-ray Crystallography," Vol. IV. Kynoch Press, Birmingham, 1974.
45. D. T. Cromer, *J. Appl. Crystallogr.* **16**, 437 (1983).
46. J. C. Phillips, J. A. Cerino, and K. O. Hodgson, *J. Appl. Crystallogr.* **12**, 592 (1979).
47. D. H. Templeton and L. K. Templeton, *Acta Crystallogr. A* **47**, 414 (1991).
48. J. A. Bearden, *Rev. Mod. Phys.* **39**, 78 (1967).
49. P. Coppens, "Synchrotron Radiation Crystallography," Academic Press, San Diego, 1992.
50. G. Materlik, C. J. Sparks, and K. Fischer, "Resonant Anomalous X-ray Scattering: Theory and Applications," North-Holland, Amsterdam, 1994.
51. T. K. Sham, *Chem. Phys. Lett.* **101**, 567 (1983).
52. J. A. Horsley, *J. Chem. Phys.* **76**, 1451 (1982).
53. F. W. Lytle, P. S. P. Wei, R. B. Gregor, G. H. Via, and J. H. Sinfelt, *J. Chem. Phys.* **70**, 4849 (1979).
54. U. W. Arndt, T. J. Greenhough, J. R. Helliwell, J. A. K. Howard, S. A. Rule, and A. W. Thompson, *Nature* **298**, 835 (1982).
55. T. J. Greenhough, J. R. Helliwell, and S. A. Rule, *J. Appl. Crystallogr.* **16**, 242 (1983).
56. K. D. Finkelstein and M. Sutton, *Nucl. Instrum. Methods Phys. Res. Sect. A* **347**, 495 (1994).